• Basic Research •

Effect of zymosan on the expression and function of the gap-junction protein connexin 43 in human corneal fibroblasts

Xiao–Shuo Zheng[1], Hui Zheng[1], Dan Xu[2], Ping–Ping Liu[1], Bing Li[1], Zi–Mu Cao[2], Yang Liu[1], Ye Liu[3]

[1]Department of Ophthalmology, the Fifth Affiliated Hospital, Sun Yat-sen University, Zhuhai 519000, Guangzhou Province, China
[2]Institute of Environmental Systems Biology, Environmental Science and Engineering College, Dalian Maritime University, Dalian 116027, Liaoning Province, China
[3]Department of Pathology, the Fifth Affiliated Hospital, Sun Yat-sen University, Zhuhai 519000, Guangzhou Province, China
Co-first authors: Xiao-Shuo Zheng and Hui Zheng
Correspondence to: Ye Liu. Department of Pathology, the Fifth Affiliated Hospital of Sun Yat-sen University, 52 Road Meihuadong, Zhuhai 519000, Guangzhou Province, China. liuye23@mail.sysu.edu.cn

Abstract
● **AIM:** To study the effect of zymosan, a ligand found on the surface of fungi, on gap junctional intercellular communication (GJIC) in cultured human corneal fibroblasts (HCFs).

● **METHODS:** Zymosan was added to the medium of cultured HCFs with or without the administration of mitogen-activated protein kinase (MAPK) inhibitors or the inhibitor kappa B kinase 2 (IKK2) inhibitor IV. The protein and mRNA levels of connexin 43 (Cx43) in HCFs were measured by Western blot, immunofluorescence, and quantitative reverse transcription-polymerase chain reaction (qRT-PCR) analyses. The GJIC activity was tested using a dye-coupling assay.

● **RESULTS:** The reduction of Cx43 protein and mRNA levels as well as a significant decrease in GJIC activity were observed in cultured HCFs when zymosan was added into the culture medium. Compared with controls (no zymosan), the protein level of Cx43 was reduced by 45% and 54% in the presence of zymosan at 200 and 600 μg/mL, respectively ($P<0.05$); and it was reduced by 45%, 48%, and 75% in the presence of zymosan (600 μg/mL) for 24, 36, and 48h, respectively ($P<0.05$). The mRNA expression of Cx43 was reduced by 98% in the presence of zymosan ($P<0.05$). The effects of zymosan on Cx43 expression and GJIC activity were attenuated by the administration of PD98059 [an extracellular signal-regulated kinase (ERK) signaling inhibitor] ($P<0.05$), c-Jun NH2-terminal kinase (JNK) inhibitor II ($P<0.05$), and IKK2 inhibitor IV ($P<0.05$).

● **CONCLUSION:** Zymosan inhibits the activity of GJIC in cultured HCFs. This effect is likely regulated *via* the nuclear factor-κB (NF-κB), MAPK/ERK, and JNK signaling pathways. The inhibitory effects of zymosan on Cx43 expression and GJIC activity in HCFs may induce damage of corneal stroma during corneal fungal infection.

● **KEYWORDS:** corneal fibroblast; zymosan; gap junction; connexin 43; MAPKs

INTRODUCTION

Fungal keratitis is a leading cause of blindness, especially in developing countries[1]. The structure of the corneal stroma and the connection of corneal fibroblasts are disrupted during fungal ulceration. However, the molecular mechanism underlying this process is not clear and further study is warranted.

It is well known that gap junctions between cells are channels for intercellular communication of secondary messengers, small metabolites, and electrical signals[2]. They are very important in cell-to-cell connectivity, tissue differentiation, and normal cell activities in organs[3]. The dysregulation and disruption of gap junction activity are causes of many diseases[4], which include corneal ulceration induced by fungal keratitis. Normally, the cornea is an avascular tissue, and the major part of it is the stroma. In the stroma, keratocytes communicate through gap junctions[5]. When the corneal stroma is disrupted, the quiescent keratocytes can be activated and differentiate into fibroblasts or myofibroblasts[6-7]. Therefore, the restoration of

functional gap junctions between differentiated fibroblasts or myofibroblasts is critical for the recovery of the cornea from fungal keratitis.

Connexins are essential proteins that form gap junctions. First, hemichannels or connexons are formed with groups of six connexins. Then two hemichannels combine together to form a gap junction[8]. Connexin-43 (Cx43) is a key gap junction protein[9]. In intestinal epithelial cells, connexin channels protect against pathogens[10]. Furthermore, in the corneal epithelium and the stroma, Cx43 expression has been detected[7,11]. In cultured corneal fibroblasts, Cx43 is expressed and forms gap junctions[7,12]. Also, inhibition or deficiency of Cx43 is associated with many disorders, *e.g.*, heart disease, cancer, skin disorders, and impaired corneal wound healing[13-17].

Zymosan is a ligand found on the surface of fungi. It activates toll-like receptor (TLR) 2 to trigger inflammatory responses in cells[9,18-19]. The activation of TLRs triggers several signaling pathways including mitogen-activated protein kinase (MAPK) and nuclear factor (NF)-κB pathways, which mediate cell activation and regulate the inflammatory response in various cells[20-21]. In our previously reported study, the expression of proinflammatory factors in cultured human corneal fibroblasts (HCFs) was induced by exposure to zymosan, and the MAPK and NF-κB pathways were involved in this process[22]. However, the effects of zymosan on gap junctions have not been reported. In the present study, we explored the effects of zymosan on Cx43 expression and gap junctional intercellular communication (GJIC) in cultured HCFs. The roles of the NF-κB and MAPK signaling pathways on the effects of zymosan on HCFs were also investigated.

MATERIALS AND METHODS

Materials Eagle's minimum essential medium (MEM), trypsin-EDTA, and fetal bovine serum (FBS) were obtained from Invitrogen-Gibco (Rockville, MD, USA). Zymosan, β-actin antibody, and bovine serum albumin (BSA) were purchased from Sigma-Aldrich (St. Louis, MO, USA). Inhibitors of MAPK signaling pathways [extracellular signal-regulated kinase (ERK) (PD98059), p38 (SB203580), and c-Jun NH2-terminal kinase (JNK; JNK inhibitor II)] and inhibitor kappa B kinase 2 (IKK2; IKK2 inhibitor IV) were purchased from Merck Millipore (Temecula, CA, USA). Molecular Probes (Eugene, OR, USA) supplied 4',6-diamidino-2-phenylindole (DAPI), Lucifer yellow CH (Li+salt), rhodamine-phalloidin, and Alexa Fluor 488-labeled antibodies (goat anti-mouse immunoglobulin G). The primary antibody against mouse Cx43 was obtained from Chemicon (Temecula, CA, USA). An enhanced chemiluminescence (ECL) kit and nitrocellulose membranes were purchased from Amersham Pharmacia Biotech (Uppsala, Sweden).

Culture of Human Corneal Fibroblasts HCFs were purchased from ScienCell Research Laboratories (cat. no. #6520; Carlsbad, CA, USA) and cultured in MEM containing 10% FBS (5% CO_2, 37℃). HCFs after four to seven generations were used in the experiments. They were collected at the sub-confluent stage and seeded into 24-well plates or culture dishes. When the cells reached confluence, the previous medium was discarded, serum-free medium (*i.e.*, MEM) was added, and the cells were cultured for an additional day. Then the cells were exposed to zymosan at 20, 60, 200, and 600 μg/mL, respectively. Zymosan (600 μg/mL) treatment of cells cultured for 6, 12, 24, 36, and 48h, respectively, was performed in some experiments. MAPK and IKK2 inhibitors at 1, 3, and 10 μmol/L were applied as interventions in some experiments. Cells not treated with zymosan were set as a control group.

Experiments Designed for the Effect of Zymosan First, the effects of zymosan on the Cx43 protein and mRNA expression levels in HCFs were examined. The impact of zymosan on the pattern of Cx43 localization in HCFs was then observed by fluorescence microscopy. In addition, the effects of MAPK inhibitors on HCFs treated with zymosan were investigated. Next, the activity of GJIC in cultured HCFs treated with or without various inhibitors was tested using a scrape-loading assay with Lucifer yellow. To study the impact of NF-κB signaling on the effect of zymosan on Cx43 expression, the IKK2 inhibitor IV, a blocker of NF-κB signaling, was administered in the medium of cultured HCFs.

Western blot Analysis The protein concentrations of Cx43 in HCFs were detected by western blot analysis[23]. The serum-deprived corneal fibroblasts were treated with or without MAPK inhibitors and IKK2 inhibitor IV, respectively, at the time of exposure or not to zymosan, for 24h. The cultured HCFs were lysed, and the protein concentration was measured by the Bradford method. Proteins were separated by sodium dodecyl sulfate-polyacrylamide gel electrophoresis and then transferred to nitrocellulose membranes. At room temperature, the membranes were blocked in a pH 7.4 solution (20 mmol/L Tris-HCl, 0.1% Tween 20, and 5% dried skim milk) for 1h, followed by overnight incubation (4℃) with Cx43 antibody (1:1000). The membranes were then rinsed four times (10min each) in washing buffer, incubated with horseradish peroxidase-conjugated secondary antibodies (room temperature, 1h), and rinsed again. ECL reagents were applied to visualize the immune complexes. The membrane was exposed to film, and the intensity of the immunoreactive bands was assessed with Image J software (NIH, Bethesda, MD, USA).

Immunofluorescence Microscopy The localization of Cx43 in HCFs was detected by immunostaining[23]. Confluent HCFs were first immersed in serum-free MEM for 24h, and then treated for another 24h with or without 600 μg/mL zymosan

(control) in serum-free MEM. The cells were fixed with ice-cold acetone for 15min. Next, 3% BSA was administered for 30min to block the nonspecific binding to antibodies. The cells were then incubated with mouse monoclonal antibody against Cx43 (dilution ratio of 1:200, room temperature) for 1h. The HCFs were further incubated with DAPI and Alexa Fluor 488-conjugated secondary antibodies (1:500, room temperature) for 1h. Images were finally obtained using a fluorescence microscope (Zeiss Axioscope, Germany).

Quantitative Reverse Transcription-Polymerase Chain Reaction The Cx43 mRNA in HCFs was measured by quantitative reverse transcription-polymerase chain reaction (qRT-PCR) analysis. Confluent HCFs were cultured in serum-free medium for 24h, and then treated for another 24h with or without 600 μg/mL zymosan (control). Total RNA was obtained from the HCFs, and qRT-PCR was performed. The sequences of the PCR primers for Cx43 cDNA and GAPDH cDNA as well as the PCR protocol were the same as those reported previously[23]. The sequences of the PCR primers were as follows: Cx43 sense, 5'-CTCGCCTATGTCTCCTCCTG-3', and Cx43 antisense, 5'-GCTGGTCCACAATGGCTAGT-3'; GAPDH sense, 5'-TGAACGGGAAGCTCACTGG-3', and GAPDH antisense, 5'-TCCACCACCCTGTTGCTGTA-3'. The PCR protocol was comprised of denaturation at 94℃ for 15s, annealing at 58℃ for 20s, and elongation at 72℃ for 13s or 15s for the amplification of Cx43 or GAPDH cDNA, respectively.

Dye Coupling Assay To reveal the functional gap junctions of corneal fibroblasts, the cell-cell transfer of Lucifer yellow was assessed. The GJIC activity was evaluated by the scrape-loading technique, as described previously[7,24], with some modifications. Serum-deprived cultured fibroblasts in 35-mm dishes were first incubated with IKK2 inhibitor IV, PD98059, or JNK inhibitor II (each at 10 μmol/L) for 1h and then treated with or without 600 μg/mL zymosan (control) for 24h. The HCFs were rinsed with divalent ion-free phosphate-buffered saline (PBS), followed by exposure to divalent ion-free PBS containing Lucifer yellow (0.5 mg/mL, room temperature). A razor blade was used to make three linear scrapes before incubation at 37℃ for 60min to let the dye easily enter into the cells. Then the cultured cells were washed three times and fixed using 4% paraformaldehyde (10min, room temperature). A fluorescence microscope (Axioscope 50, Zeiss) was used to observe the fixed HCFs. The average maximal distance was used to determine the extent of spreading of the Lucifer yellow among the cells. ImageJ software (NIH, Bethesda, MD, USA) was used to evaluate the dye fluorescence. For each scrape line, at least three measurements were collected and analyzed.

**Statistical Analysis** SPSS (version V20.0, IBM, New York, NY, USA) was applied for the statistical analyses in this study. Descriptive data were expressed as the mean±standard deviation. Comparisons between the case and control groups were performed using the Student's *t*-test or Dunnett's multiple comparison test. Data for each group were obtained from at least three independent samples, and all sampling was repeated three times for the study groups. The statistical significance was set as $P<0.05$.

RESULTS

Impact of Zymosan on Cx43 Expression Western blot analysis revealed a concentration-dependent reduction of Cx43 expression when the corneal fibroblasts were treated with zymosan at four different concentrations (20, 60, 200, and 600 μg/mL) for 24h (Figure 1A). Starting at a concentration of 200 μg/mL, zymosan treatment showed a significant inhibitory effect, and the maximal effect was observed at a concentration of 600 μg/mL (Figure 1B). The relative Cx43 band intensities were 1.78±0.10, 1.89±0.14, 1.51±0.09, 0.98±0.20, and 0.81±0.14 at zymosan concentrations of 0, 20, 60, 200, and 600 μg/mL, respectively. The expression of Cx43 was inhibited by 45% and 54% in the presence of zymosan at 200 and 600 μg/mL, respectively. Moreover, zymosan (600 μg/mL) treatment reduced the Cx43 expression level in a time-dependent manner (Figure 2A); the inhibitory effect was statistically significant beginning at an exposure time of 24h (Figure 2B). The relative Cx43 band intensities were 2.45±0.12, 1.99±0.13, 1.86±0.02, 1.34±0.27, 1.28±0.07, and 0.62±0.20 at exposure times of 0, 6, 12, 24, 36, and 48h, respectively. The expression of Cx43 was inhibited by 45%, 48%, and 75% in the presence of zymosan (600 μg/mL) for 24, 36, and 48h, respectively.

In the control cells, Cx43 was stained specifically and showed a punctate pattern of fluorescence. Under a microscope, the quantity of punctate fluorescence was markedly reduced in the fibroblasts exposed to zymosan (Figure 3). In addition, qRT-PCR revealed that Cx43 expression was significantly reduced in the cultured corneal fibroblasts exposed to zymosan (600 μg/mL) for 24h (Figure 4). The mRNA expression of Cx43 was inhibited by 98% in the presence of zymosan (600 μg/mL).

Role of MAPK Signaling on the Impact of Zymosan on Cx43 Expression The reduction of Cx43 expression in the HCFs treated with zymosan was shown by Western blot analysis. The reduction was inhibited by the addition of PD98059 and JNK inhibitor II, respectively, in a concentration-dependent manner; however, such an effect was not observed with SB203580 treatment (Figure 5). The relative Cx43 band intensities were 4.09±0.51 in the absence of zymosan, and 1.60±0.10, 2.12±0.29, 2.37±0.15, and 3.00±0.20 at PD98059 concentrations of 0, 1, 3, and 10 μmol/L in the presence of 600 μg/mL zymosan, respectively (Figure 5A). The relative Cx43 band intensities were 3.82±0.27 in the absence of
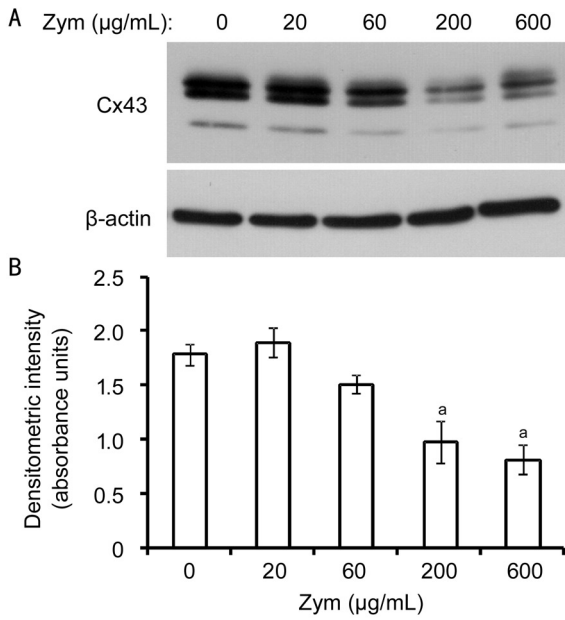
Figure 1 Concentration-dependent inhibitory effect of zymosan (Zym) on Cx43 expression in cultured HCFs A: After exposure of HCFs to various concentrations of zymosan, the expression of Cx43 was examined by Western blot analysis; B: The immunoblots were subjected to densitometric analysis in order to determine the band intensity. The error bars represent the standard deviation. [a]$P<0.05$ (Dunnett's multiple comparison test) versus the control (no zymosan).
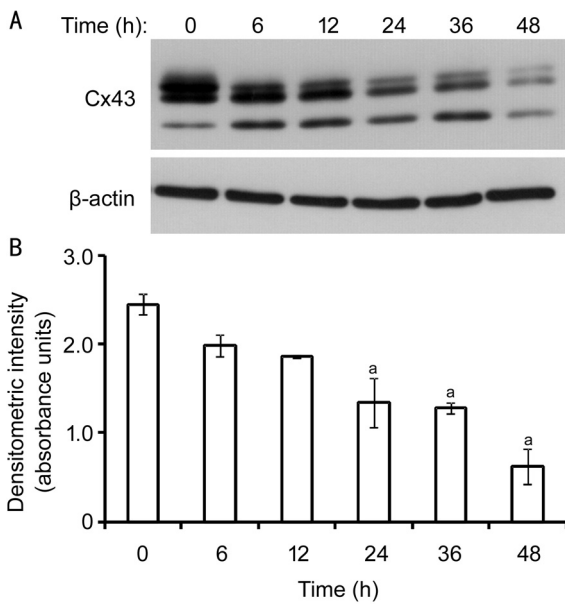

Figure 2 Time-dependent inhibitory effect of zymosan on Cx43 expression in cultured HCFs A: After the exposure of HCFs to zymosan (600 μg/mL) for the indicated time, the expression of Cx43 was examined by Western blot analysis; B: The immunoblots were subjected to densitometric analysis in order to determine the band intensity. The error bars represent the standard deviation. [a]$P<0.05$ (Dunnett's multiple comparison test) versus the control (no zymosan).

zymosan, and 1.81±0.47, 1.09±0.28, 1.12±0.20, and 1.25±0.38 at SB203580 concentrations of 0, 1, 3, and 10 μmol/L in the presence of 600 μg/mL zymosan, respectively (Figure 5B). The
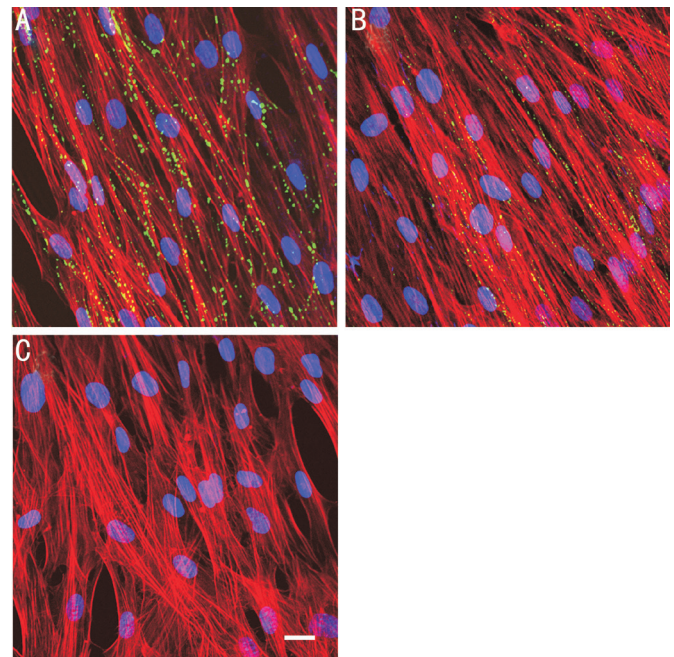

Figure 3 Effect of zymosan on the distribution of Cx43 expression in cultured HCFs Serum-deprived cells were treated with nothing (A) or zymosan (600 μg/mL) (B, C) for 24h. The cells were stained with antibodies against Cx43 (A, B) or a normal mouse IgG (C), and then stained with Alexa Fluor 488-conjugated secondary antibodies (green color), rhodamine-phalloidin (red color, F-actin), and DAPI (blue color, nuclei). Scale bar, 50 μm.
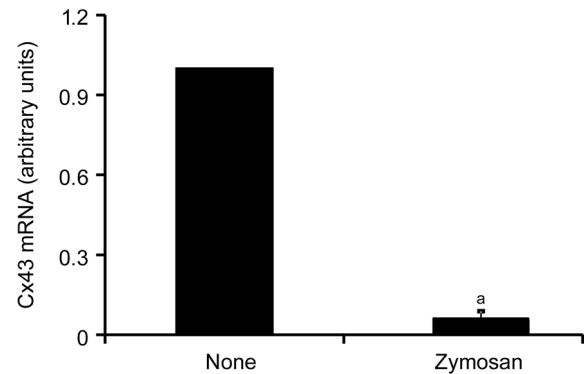
Figure 4 Effect of zymosan on the abundance of Cx43 mRNA in cultured HCFs After HCFs were incubated with or without zymosan (600 μg/mL) for 24h, the Cx43 mRNA level in the cells was then determined by qRT-PCR analysis. The error bars represent the standard deviation. [a]$P<0.05$ (Student's t-test) versus the control (no zymosan).

relative Cx43 band intensities were 4.16±0.40 in the absence of zymosan, and 1.72±0.23, 1.64±0.71, 2.55±0.38, and 3.12±0.29 at JNK inhibitor II concentrations of 0, 1, 3, and 10 μmol/L in the presence of 600 μg/mL zymosan, respectively (Figure 5C). The inhibitory effect of zymosan on Cx43 expression was attenuated by 13%, 19%, and 34% in the presence of PD98059 at concentrations of 1, 3, and 10 μmol/L, respectively; and it was attenuated by 20% and 34% in the presence of JNK inhibitor II at concentrations of 3 and 10 μmol/L, respectively.
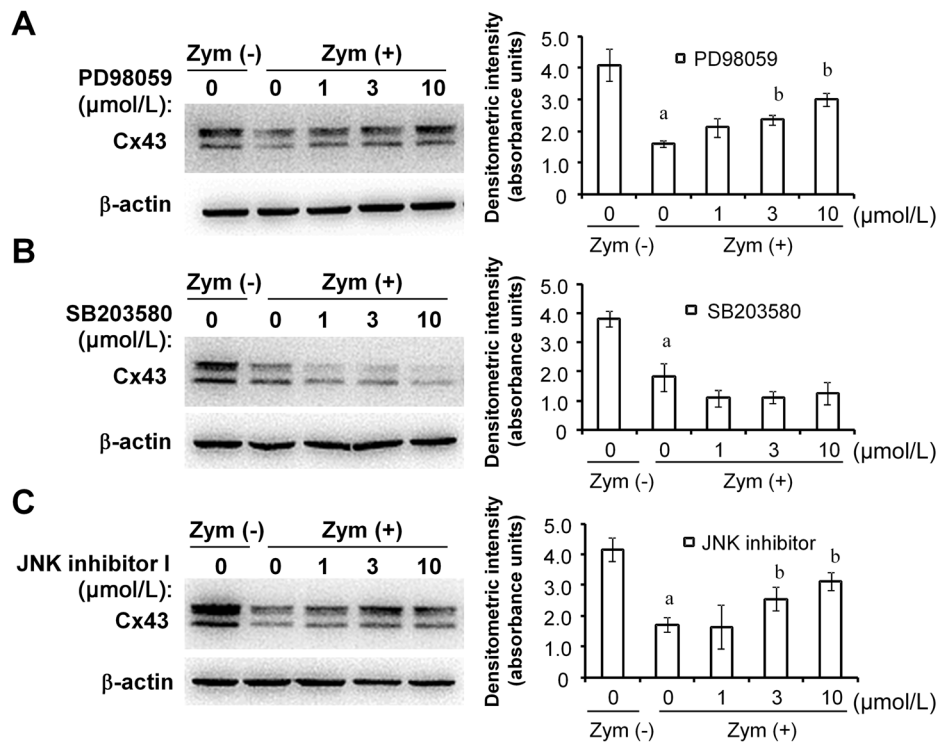
Figure 5 Effects of MAPK signaling inhibitors on the zymosan-induced downregulation of Cx43 expression in cultured HCFs A: After HCFs were treated with PD98059, SB203580, or JNK inhibitor II (at 1, 3, and 10 μmol/L), respectively, in the absence or presence of zymosan (600 μg/mL), the expression of Cx43 was then examined by Western blot analysis; B: Densitometric analysis was performed for the immunoblots to determine the band intensity. The error bars represent the standard deviation. [a]$P<0.05$ (Dunnett's test) versus the control (no zymosan); [b]$P<0.05$ (Dunnett's test) versus the corresponding control (zymosan only).
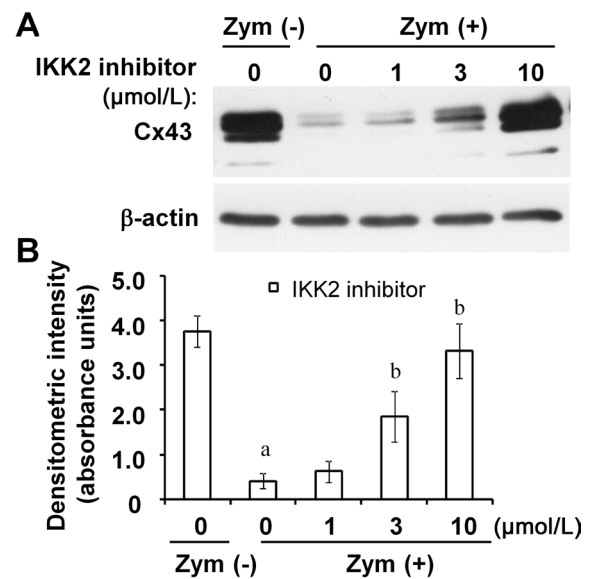
Impact of NF-κB Signaling on the Effect of Zymosan on Cx43 Expression The reduction of Cx43 expression, which was induced by zymosan treatment, in the cultured HCFs was offset by IKK2 inhibitor IV administration. According to Western blot analysis, the inhibitory effect of IKK2 inhibitor IV occurred in a concentration-dependent manner (Figure 6). The relative Cx43 band intensities were 3.77±0.35 in the absence of zymosan, and 0.40±0.17, 0.63±0.24, 1.85±0.56, and 3.33±0.61 at IKK2 inhibitor IV concentrations of 0, 1, 3, and 10 μmol/L in the presence of 600 μg/mL zymosan, respectively. The inhibitory effect of zymosan on Cx43 expression was attenuated by 6%, 39%, and 78% in the presence of IKK2 inhibitor IV at concentrations of 1, 3, and 10 μmol/L, respectively.
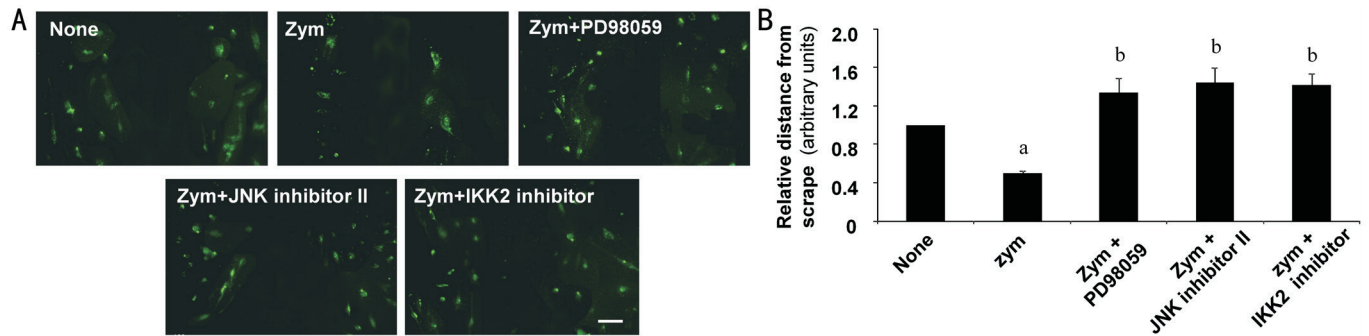
Effect of Zymosan on GJIC Activity in HCFs A significant reduction of dye coupling in HCFs was observed after a 24-h incubation with zymosan (600 μg/mL). IKK2 inhibitor IV, PD98059, or JNK inhibitor II (10 μmol/L) significantly offset the effect of zymosan on GJIC activity in HCFs (Figure 7A). The relative distances from the scrape were 1.00±0.00 and 0.45±0.12 in the absence or presence of zymosan, and 1.25±0.27, 1.34±0.31, and 1.28±0.25 in the presence of PD98059, JNK inhibitor II, or IKK2 inhibitor IV combined with zymosan, respectively (Figure 7B).

DISCUSSION

In the present study, the inhibition of Cx43 expression and

Figure 6 Effect of the NF-κB signaling inhibitor on the zymosan-induced downregulation of Cx43 expression in cultured HCFs A: HCFs were treated with IKK2 inhibitor IV (1, 3, and 10 μmol/L) in the absence or presence of zymosan (600 μg/mL). The expression of Cx43 was then examined by Western blot analysis. B: The immunoblots were subjected to densitometric analysis in order to determine the band intensity. The error bars represent the standard deviation. [a]$P<0.05$ (Dunnett's test) versus the control (no zymosan). [b]$P<0.05$ (Dunnett's test) versus the corresponding control (zymosan only).

Figure 7 Effect of zymosan on gap junctional intercellular communication (GJIC) activity in cultured HCFs HCFs were treated with the ERK inhibitor PD98059, JNK inhibitor II, or IKK2 inhibitor IV (10 μmol/L), respectively, in the absence or presence of zymosan (600 μg/mL). A scrape-loading assay with Lucifer yellow was used to measure the GJIC activity. A: Representative fluorescence microscopy images of fixed cells from different treatments (scale bar, 100 μm); B: The maximum distances from the scrape to dye fluorescence were quantified to show the GJIC activity. The error bars represent the standard deviation. [a]$P<0.05$ (Dunnett's test) versus the control (no zymosan). [b]$P<0.05$ (Dunnett's test) versus the corresponding control (zymosan only).

GJIC activity was observed in cultured HCFs incubated with zymosan. Furthermore, the effects of zymosan on the cultured HCFs were attenuated by the administration of the ERK inhibitor PD98059, JNK inhibitor II, and IKK2 inhibitor IV, respectively. Inflammation is a double-edged sword that protects tissues and cells during pathogenesis and causes cell damage when the reaction is excessive. Cx43 plays a role in mediating inflammation and is involved in the release of cytokines and immunoglobulins[25]. In addition, Cx43 expression is important for the normal function of the eye, and it is observed in the pathogenesis as well, *e.g.*, corneal infection and wound healing[26]. Alteration in the Cx43 level has been found in corneal infection and chemical burns[27]. Moreover, Gap27, a Cx43 mimetic peptide, has demonstrated an inhibitory effect on the gap junction function. For example, treatment of rat corneas with Gap27 after deep stromal injury resulted in an increased rate of early granulocyte infiltration and late gene expression of tumor necrosis factor (TNF)-α and tissue growth factor (TGF)-β1[16], which are the key molecules involved in the processes of inflammation and wound healing. As a component of the fungal yeast wall, zymosan is a critical factor that induces inflammation and has been used as a phagocytic stimulus for *in vitro* studies. In the present study, zymosan reduced Cx43 expression and GJIC activity, suggesting that zymosan plays a role in the corneal inflammatory process of fungal infection. As reported previously, zymosan induces the production of proinflammatory factors, such as monocyte chemoattractant protein-1, interleukin-8, and interleukin-6 in HCFs[22], as well as the expression of matrix metalloproteinases in corneal epithelial cells[19]. It is still a challenging issue to control the inflammation in the corneal stroma for patients with fungal keratitis. Based on the results from the present study, we postulate that zymosan aggravates the inflammatory reaction in the corneal stroma by regulating the function of

corneal fibroblasts, therefore inducing excessive inflammatory damage to the cornea during fungal infection. Since the absence of cell-cell contact is a precondition for fibroblasts to differentiate into myofibroblasts induced by TGF, and the absence of communication between cells leads to excessive cell proliferation and fibrosis[28-29], the reduction of GJIC activity in HCFs by zymosan shown in the present study may contribute to corneal scar formation during fungal infection. However, future studies assessing the correlation between Cx43 levels and fungal keratitis are warranted.

TLRs belong to the group of pattern recognition receptors and are crucial in the host inflammatory response during an infection. The levels of proinflammatory factors in immune cells are increased when zymosan binds to TLR2 on the cells[30]. TLRs are activated and then trigger signaling pathways, such as MAPK (p38, JNK, and ERK) pathways. In the present study, we found that PD85098 and JNK inhibitor II attenuated the effects of zymosan on the cultured HCFs. However, the p38 inhibitor did not show the same effect on Cx43 expression and GJIC activity. These findings suggest that phosphorylation of MAPK/JNK and ERK is involved in the effects of zymosan on HCFs. It has been reported that alteration of the Cx43 level in keratinocytes and mammary glands induced by TGF-β or TNF-α is offset by JNK and p38[31-32]. In addition, during *Pseudomonas aeruginosa* infection of airway epithelial cells, the Cx43 level was upregulated by p38; whereas JNK downregulated Cx43 expression in these cells[10]. However, in atrial myocytes, ERK activation is involved in the Cx43 expression reduction caused by macrophage migration inhibitory factor[33]. These studies suggest that Cx43 expression might be differentially regulated by MAPKs in different cell types and disorders.

Besides the MAPK pathway, activation of TLR2 triggers NF-κB signaling. NF-κB is located in the cytoplasm when it is not

activated, and it forms a structure bound to the inhibitory protein IκB. When NF-κB is activated by zymsoan, IκB is phosphorylated, followed by ubiquitination and degradation. Consequently, NF-κB is released to the nucleus and activates the downstream promoters[19]. We have shown previously that zymosan induces the activation and degradation of IκB-α in cultured HCFs[22]. In the present research, IKK2 inhibitor IV attenuated the effect of zymosan on GJIC activity and Cx43 expression in HCFs. Therefore, suppression of NF-κB could also be a mechanism explaining the effects of zymosan on HCFs.

In summary, we have shown that zymosan suppressed the GJIC activity and Cx43 expression in cultured HCFs. The effects were possibly regulated by the NF-κB, MAPK/ERK, and JNK signaling pathways. The downregulation of GJIC among corneal fibroblasts induced by zymosan plays a role in the damage of corneal stroma when the cornea suffers a fungal infection.

ACKNOWLEDGEMENTS

Conflicts of Interest: Zheng XS, None; **Zheng H,** None; **Xu D,** None; **Liu PP,** None; **Li B,** None; **Cao ZM,** None; **Liu Y,** None; **Liu Y,** None.

REFERENCES

1 Lalitha P, Prajna NV, Manoharan G, Srinivasan M, Mascarenhas J, Das M, D'Silva SS, Porco TC, Keenan JD. Trends in bacterial and fungal keratitis in South India, 2002-2012. *Br J Ophthalmol* 2015;99(2):192-194.

2 Beyer EC, Berthoud VM. Gap junction gene and protein families: Connexins, innexins, and pannexins. *Biochim Biophys Acta Biomembr* 2018;1860(1):5-8.

3 Papaneophytou C, Georgiou E, Kleopa KA. The role of oligodendrocyte gap junctions in neuroinflammation. *Channels (Austin)* 2019;13(1): 247-263.

4 Sánchez A, Castro C, Flores DL, Gutiérrez E, Baldi P. Gap junction channels of innexins and connexins: relations and computational perspectives. *Int J Mol Sci* 2019;20(10):2476.

5 Laux-Fenton WT, Donaldson PJ, Kistler J, Green CR. Connexin expression patterns in the rat cornea: molecular evidence for communication compartments. *Cornea* 2003;22(5):457-464.

6 Torricelli AAM, Santhanam A, Wu JH, Singh V, Wilson SE. The corneal fibrosis response to epithelial-stromal injury. *Exp Eye Res* 2016;142:110-118.

7 Spanakis SG, Petridou S, Masur SK. Functional gap junctions in corneal fibroblasts and myofibroblasts. *Invest Ophthalmol Vis Sci* 1998;39(8):1320-1328.

8 Totland MZ, Rasmussen NL, Knudsen LM, Leithe E. Regulation of gap junction intercellular communication by connexin ubiquitination: physiological and pathophysiological implications. *Cell Mol Life Sci* 2020;77(4):573-591.

9 Chen MJ, Kress B, Han X, Moll K, Peng W, Ji RR, Nedergaard M. Astrocytic CX43 hemichannels and gap junctions play a crucial role in development of chronic neuropathic pain following spinal cord injury. *Glia* 2012;60(11):1660-1670.

10 Losa D, Köhler T, Bellec J, Dudez T, Crespin S, Bacchetta M, Boulanger P, Hong SS, Morel S, Nguyen TH, van Delden C, Chanson M. *Pseudomonas aeruginosa*-induced apoptosis in airway epithelial cells is mediated by gap junctional communication in a JNK-dependent manner. *J Immunol* 2014;192(10):4804-4812.

11 Lu X, Chen Z, Vick S, Watsky MA. Vitamin D receptor and metabolite effects on corneal epithelial cell gap junction proteins. *Exp Eye Res* 2019;187:107776.

12 Petridou S, Masur SK. Immunodetection of connexins and cadherins in corneal fibroblasts and myofibroblasts. *Invest Ophthalmol Vis Sci* 1996;37(9):1740-1748.

13 Akar FG, Nass RD, Hahn S, Cingolani E, Shah M, Hesketh GG, DiSilvestre D, Tunin RS, Kass DA, Tomaselli GF. Dynamic changes in conduction velocity and gap junction properties during development of pacing-induced heart failure. *Am J Physiol Heart Circ Physiol* 2007;293(2):H1223-H1230.

14 Lilly E, Sellitto C, Milstone LM, White TW. Connexin channels in congenital skin disorders. *Semin Cell Dev Biol* 2016;50:4-12.

15 Tschernig T. Connexins and gap junctions in cancer of the urinary tract. *Cancers (Basel)* 2019;11(5):704.

16 Elbadawy HM, Mirabelli P, Xeroudaki M, Parekh M, Bertolin M, Breda C, Cagini C, Ponzin D, Lagali N, Ferrari S. Effect of connexin 43 inhibition by the mimetic peptide Gap27 on corneal wound healing, inflammation and neovascularization. *Br J Pharmacol* 2016;173(19):2880-2893.

17 Zieske JD. Extracellular matrix and wound healing. *Curr Opin Ophthalmol* 2001;12(4):237-241.

18 Jiang LI, Sternweis PC, Wang JE. Zymosan activates protein kinase A via adenylyl cyclase VII to modulate innate immune responses during inflammation. *Mol Immunol* 2013;54(1):14-22.

19 Li DQ, Zhou N, Zhang L, Ma P, Pflugfelder SC. Suppressive effects of azithromycin on zymosan-induced production of proinflammatory mediators by human corneal epithelial cells. *Invest Ophthalmol Vis Sci* 2010;51(11):5623-5629.

20 Roshan MHK, Tambo A, Pace NP. The role of TLR2, TLR4, and TLR9 in the pathogenesis of atherosclerosis. *Int J Inflam* 2016;2016: 1532832.

21 Akhtar M, Shaukat A, Zahoor A, Chen Y, Wang Y, Yang M, Umar T, Guo M, Deng G. Hederacoside-C inhibition of *Staphylococcus aureus*-induced mastitis via TLR2 & TLR4 and their downstream signaling NF-κB and MAPKs pathways *in vivo* and *in vitro*. *Inflammation* 2020;43(2):579-594.

22 Liu Y, Li J, Liu Y, Wang P, Jia H. Inhibition of zymosan-induced cytokine and chemokine expression in human corneal fibroblasts by triptolide. *Int J Ophthalmol* 2016;9(1):9-14.

23 Kimura K, Nishida T. Role of the ubiquitin-proteasome pathway in downregulation of the gap-junction protein Connexin43 by TNF-α in human corneal fibroblasts. *Invest Ophthalmol Vis Sci* 2010;51(4): 1943-1947.

24 Zhao Y, Rivieccio MA, Lutz S, Scemes E, Brosnan CF. The TLR3 ligand polyI: C downregulates connexin 43 expression and function in astrocytes by a mechanism involving the NF-κB and PI3 kinase pathways. *Glia* 2006;54(8):775-785.

25 Oviedo-Orta E, Howard Evans W. Gap junctions and connexin-mediated communication in the immune system. *Biochim Biophys Acta* 2004;1662(1-2):102-112.

26 Xu CY, Zhang WS, Zhang H, Cao Y, Zhou HY. The role of connexin-43 in the inflammatory process: a new potential therapy to influence keratitis. *J Ophthalmol* 2019;2019:9312827.

27 Zhai J, Wang Q, Tao L. Connexin expression patterns in diseased human corneas. *Exp Ther Med* 2014;7(4):791-798.

28 Masur SK, Dewal HS, Dinh TT, Erenburg I, Petridou S. Myofibroblasts differentiate from fibroblasts when plated at low density. *Proc Natl Acad Sci U S A* 1996;93(9):4219-4223.

29 Kumar NM, Gilula NB. The gap junction communication channel. *Cell* 1996;84(3):381-388.

30 Nohmi K, Tokuhara D, Tachibana D, Saito M, Sakashita Y, Nakano A, Terada H, Katayama H, Koyama M, Shintaku H. Zymosan induces immune responses comparable with those of adults in monocytes, dendritic cells, and monocyte-derived dendritic cells from cord blood. *J Pediatr* 2015;167(1):155-162.e1-2.

31 Tacheau C, Fontaine J, Loy J, Mauviel A, Verrecchia F. TGF-b induces connexin43 gene expression in normal murine mammary gland epithelial cells via activation of p38 and PI3K/AKT signaling pathways. *J Cell Physiol* 2008;217(3):759-768.

32 Tacheau C, Laboureau J, Mauviel A, Verrecchia F. TNF-α represses connexin43 expression in HaCat keratinocytes via activation of JNK signaling. *J Cell Physiol* 2008;216(2):438-444.

33 Li X, Rao F, Deng CY, Wei W, Liu FZ, Yang H, Wang ZY, Kuang SJ, Chen XY, Xue YM, Wu SL. Involvement of ERK1/2 in Cx43 depression induced by macrophage migration inhibitory factor in atrial myocytes. *Clin Exp Pharmacol Physiol* 2017;44(7):771-778.